Int. J. Cancer: **121,** 1670–1679 (2007)

Gossypol reduction of tumor growth through ROS-dependent mitochondria pathway in human colorectal carcinoma cells

Ching-Huai Ko[1], Shing-Chuan Shen[2,3], Liang-Yo Yang[4], Cheng-Wei Lin[1] and Yen-Chou Chen[5,6]*

[1]*Graduate Institute of Pharmacy, School of Pharmacy, Taipei Medical University, Taipei, Taiwan*
[2]*Department of Dermatology, School of Medicine, Taipei Medical University, Taipei, Taiwan*
[3]*Department of Dermatology, Taipei Municipal Wan-Fang Hospital, Taipei, Taiwan*
[4]*Department of Physiology and Graduate Institute of Neuroscience, Taipei Medical University, Taipei, Taiwan*
[5]*Graduate Institute of Pharmacognosy, School of Pharmacy, Taipei Medical University, Taipei, Taiwan*
[6]*Topnotch Stroke Research Center, Taipei Medial University, Taipei, Taiwan*

Among 13 different cell lines, gossypol (GOS) showed the most potent cytotoxic effect against human colorectal carcinoma cells including HT29, COLO205, COLO320HSR and COLO320DM cells according to an MTT assay. The cytotoxic effect of GOS was mediated by its induction of apoptosis as characterized by the occurrence of DNA ladders, apoptotic bodies and chromosome condensation in both COLO205 and HT29 cells. Activation of caspase 3, 6, 8 and 9, but not caspase 1, accompanied by the appearance of cleaved fragments of PARP (85 kDa), and caspase 3 (p17/p15), was identified in GOS-treated cells. Decreases in Bcl-xL and phosphorylated Bad proteins were found in GOS-treated cells. GOS induction of ROS production was detected by *in vitro* plasmid digestion, and an increase in the intracellular peroxide level was observed in GOS-treated COLO205 cells by the DCHF-DA assay. Antioxidants including *N*-acetyl-L-cysteine (NAC), catalase (CAT), tempol (TEM) and melatonin (MEL), but not allopurinol (ALL), pyrrolidine dithiocarbamate (PDTC) or diphenylene iodonium (DPI), significantly inhibited GOS-induced Reactive oxygen species (ROS) production through blocking the occurrence of apoptosis. GOS induced mitochondrial dysfunction characterized by a loss of the mitochondria membrane potential via DiOC6 staining, and the release of cytochrome c (Cyt c) and apoptosis-inducing factor (AIF) from mitochondria to the cytoplasm was observed. Removing mitochondria by ethidium bromide (EtBr) treatment significantly reduced the apoptotic effect of GOS in COLO205 cells. Furthermore, an intraperitoneal injection of GOS or gossypol acetic acid (GAA) significantly reduced the growth of colorectal carcinoma induced by a subcutaneous injection of COLO205 cells in nude mice. Results of the present study provide the first evidences demonstrating the *in vitro* and *in vivo* antitumor effects of GOS via an ROS-dependent mitochondrial apoptosis in colorectal carcinoma.

Key words: gossypol; apoptosis; reactive oxygen species; mitochondria; cytochrome c; apoptosis-inducing factor

Gossypol (GOS) is a polyphenolic compound isolated from cotton seeds, and has been successfully used as a male contraceptive drug for many years.[1] Several proposed clinical applications of GOS have been reported including antiviral, antimalarial and antitumor effects.[2–4] Recent observations have suggested the antiproliferative and antimetastatic activities of GOS in several tumor cells including leukemia cells, colon carcinoma cells, glioma cells and prostate carcinoma cells.[5,6] The clinical research of GOS has shown that GOS inhibits the metastasis of adrenal carcinoma, malignant glioma and breast carcinoma.[7–9] However, information on the molecular mechanism of GOS-induced antitumor effect is still limited.

Both cell cycle arrest and cell death have been reported in GOS-treated cells, and several previous studies indicated that GOS-induced cell death occurs through apoptosis.[3,5] In rat spermatocytes, GOS-induced apoptosis is mediated by the biphasic induction of c-Myc protein in accordance with stimulation of c-fos gene expression.[10] Tseng *et al*. suggested that GOS-induced apoptotic DNA fragmentation in spermatocytes was correlated with the blocking of protein kinase C (PKC) activity.[11] In addition to spermatocytes, GOS has been shown to inhibit DNA synthesis and induce DNA breaks or DNA fragmentation in tumor cells *in vitro*. GOS has been demonstrated to block the binding of Bcl-2 and Bcl-$_{XL}$ to pro-apoptotic Bcl-2 family proteins such as Bim and Bad via interacting with their BH3 domain.[3,12] In human A549 lung alveolar lung cancer cells, an increase in the Fas/FasL apoptotic pathway, but not the p53-p21 pathway, was involved in GOS-induced apoptosis.[13] Another important benefit of GOS is its safety and stimulatory apoptotic effect on drug resistant cancer cells. Oliver *et al*. indicated that GOS acts directly on mitochondria to overcome Bcl-2 and Bcl-$_{XL}$-induced apoptosis resistance.[12] Xu *et al*. indicated that GOS induces tumor regression via enhancing the response to radiation therapy in human prostate cancer.[6] Hu *et al*. indicated that milk derived from GOS-treated cows exhibited antineoplastic activity.[14] These data suggest that GOS is an effective antitumor agent with developmental potential.

Mitochondria are important organelles in apoptosis induction, and mitochondria which become permeable and release apoptotic protein cytochrome c (Cyt c) or apoptosis-inducing factor (AIF) from the mitochondrial intermembrane to the cytosol have been identified in apoptosis.[15,16] Release of Cyt c from mitochondria can activate caspase 9, which in turn activates executioner caspase 3 via cleavage induction. Some substrates for caspase 3 such as poly(ADP-ribose) polymerase are cleaved, leading to apoptosis.[17] Several studies have indicated that reactive oxygen species (ROS) may mediate apoptosis induction, and many stimuli such as tumor necrosis factor-α, and etoposide induce apoptosis induce apoptosis via stimulating ROS production.[18,19] Hou *et al*. indicated that GOS induces apoptosis through an ROS-independent mitochondria pathway in human leukemia HL-60 cells.[20] However, the roles of ROS and mitochondria in GOS-induced apoptosis are still undefined.

In the present study, we found that GOS preferentially induced cell death in colorectal carcinoma cells (COLO205, HT29, COLO320HSR and COLO320DM), but was less sensitive in embryonic NIH3T3 fibroblasts, macrophages (RAW264.7 and J774A.1), human leukemia cells (HL60 and Jurkat), epidermoid A431 cells, HaCaT keratinocytes and glioma cells C6. GOS-induced apoptosis via an ROS-dependent mitochondria pathway was identified in

Abbreviations: AIF, apoptosis-inducing factor; ALL, allopurinol; BCIP, 5-bromo-4-chloro-3-indolyl-phosphate; Bcl-2, B-cell lymphoma-2; CAT, catalase; Cyt c, cytochrome c; DCHF-DA, dichlorodihydrofluorescein diacetate; DPI, diphenylene iodonium; EtBr, ethidium bromide; GAA, gossypol acetic acid; GOS, gossypol; MEL, melatonin; NAC, *N*-acetyl-L-cysteine; NBT, nitro blue tetrazolium; PDTC, pyrrolidine dithiocarbamate; ROS, reactive oxygen species; TEM, tempol.

Grant sponsor: National Science Council of Taiwan; Grant numbers: NSC94-2320-B-038-049, 95-3112-B-038-003 and 93-2320-B-038-029-MY2; Grant sponsor: Topnotch Stroke Research Center Grant, Ministry of Education.

***Correspondence to:** Yen-Chou Chen, Taipei Medial University, Taipei, Taiwan. Fax: +886-2-23787139. E-mail: yc3270@tmu.edu.tw

Received 14 December 2006; Accepted after revision 8 May 2007
DOI 10.1002/ijc.22910
Published online 27 June 2007 in Wiley InterScience (www.interscience.wiley.com).

human colorectal carcinoma cells. Furthermore, the *in vivo* anticolorectal carcinoma effect of GOS was investigated.

Material and methods

Cell culture

The HT29, COLO205, COLO320HSR, COLO320DM, HL-60, Jurkat, RAW264.7, J774A.1, NIH3T3, A431, HaCaT, glioma C6 and MCF-7 cell lines were obtained from American Type Culture Collection (ATCC; Rockville, MD). COLO205-X cells were primary-cultured cells from tumor tissues elicited by injecting COLO205 cells into nude mice. HT29, COLO205, COLO320HSR, COLO320DM and HL-60 cells were grown in RPMI1640 containing 10% heat-inactivated fetal bovine serum (FBS); Jurkat, RAW264.7, J774A.1, NIH3T3, A431, HaCaT, Glioma C6 and MCF-7 cells were grown in DMEM containing 10% heat-inactivated FBS (fetal bovine serum), and were maintained at 37°C in a humidified incubator containing 5% CO_2. All cultured reagents were purchased from Gibco/BRL (Grand Island, NY).

Chemicals

GOS and gossypol acetic acid (GAA) were purchased from Sigma Chemical (St. Louis, MO). For *in vitro* study, GOS and GAA are dissolved in DMSO at the stock dose of 10 mM. For *in vivo* study, GOS and GAA are dissolved in 20% DMSO at the dose of 100 mg/ml, and dilution of GOS and GAA to working doses (5 and 10 mg/kg) was performed by adding sterilized PBS. The colorigenic synthetic peptide substrates, Ac-DEVD-pNA, Ac-YVAD-pNA, Ac-IETD-pNA, Ac-VEID-pNA and Ac-LEHD-pNA and the protease inhibitors, Z-VAD-FMK, Ac-DEVD-FMK, Ac-YVAD-FMK, Ac-VEID-FMK, Ac-IETD-FMK and Ac-LEHD-FMK were purchased from Calbiochem (La Jolla, CA). Dichlorodihydrofluorescein diacetate (DCHF-DA) and DiOC6(3) were obtained from Molecular Probe (Eugene, OR). Propidium iodide (PI), N-acetyl-L-cysteine (NAC), catalase (CAT), allopurinol (ALL), pyrrolidine dithiocarbamate (PDTC), diphenylene iodonium (DPI), tempol (TEM), melatonin (MEL) and other chemicals were obtained from Sigma Chemical (St. Louis, MO). NAC was dissolved in PBS, followed by adjustment of the pH value to 7.0 by adding 1 M NaOH. The stock concentration of NAC is 500 mM and sterilized by 0.22 μM filtration. Antibodies for Western blotting including antiAIF, anticaspase 6, anticaspase 8 and anticaspase 9 were obtained from Cell Signaling Technology (Danvers, MA). AntiPARP and anticaspase 3 were obtained from IMGENEX Corporation (San Diego, CA). Antibodies for cytochrome c, Bcl-2 family proteins and α-tubulin were purchased from Santa Cruz Biotech (Santa Cruz, CA).

Cell viability

Cell viability was assessed by MTT staining as described by Ko *et al*.[21] Cells were plated at a density of 1×10^6 cells/well in 24-well plates for 24 hr, and treated with different concentration of GOS for 24 hr. At the end of treatment, 30 μl of the tetrazolium compound, 3-(4,5-dimethylthiazol-2-yl)-2,5-diphenyl tetrazolium bromide (MTT) and 270 μl of fresh RPMI medium were added for 4 hr at 37°C. The formazan crystals were dissolved by DMSO, and the absorbance at a wavelength of 600 nm was recorded using an ELISA plate reader.

DNA fragmentation assay

Cells (10^6/ml) under different treatments were collected, washed with PBS twice, then lysed in 100 μl of lysis buffer (50 mM Tris (pH 8.0), 10 mM ethylenediaminetetraacetic acid (EDTA), 0.5% sodium sarkosinate and 1 mg/ml proteinase K) for 3 hr at 56°C and then treated with 0.5 mg/ml RNase A for another hour at 56°C. DNA was extracted with phenol/chloroform/isoamyl alcohol (25/24/1 v/v) before loading. An equal amount of DNA (1 μg/lane) derived from each sample was mixed with loading buffer (50 mM Tris, 10 mM EDTA, 1% (w/w) low-melting-point agarose and 0.025% (w/w) bromophenol blue) and loaded onto a pre-solidified 2% agarose gel containing 0.1 μg/ml ethidium bromide (EtBr). The agarose gels were run at 50 V for 90 min in TBE buffer, then observed and photographed under UV light.

Western blotting

Total cellular proteins (30 μg) derived from cells under different treatments were prepared, and separated on 8% SDS-polyacrylamide mini gels for PARP detection and 12% for SDS-polyacrylamide mini gels for caspase 3, Bcl-2 family proteins and α-tubulin detection. Expression of the indicated protein was visualized by incubating with the colorimetric substrates, nitro blue tetrazolium (NBT) and 5-bromo-4-chloro-3-indolyl-phosphate (BCIP), as described in our previous paper.[22]

Release of cytochrome c and AIF from mitochondria in GOS-treated cells

Untreated and drug-treated cells were harvested by centrifugation at 1,000*g* for 5 min at 4°C. The cells pellets were washed once with ice-cold PBS and resuspended in 5 volumes of 20 mM HEPES-KOH (pH 7.5), 10 mM KCl, 1.5 mM $MgCl_2$, 1 mM EDTA, 1 mM EGTA, 1 mM DTT, 0.1 mM PMSF and 250 mM sucrose. Cells were homogenized and centrifuged at 750*g* for 10 min at 4°C. The supernatants were then centrifuged at 10,000*g* for 15 min at 4°C. The pellets were lysed with 0.1 ml of lysis buffer consisting of 10 mM Tris-HCl (pH 7.4), 1 mM EDTA, 1 mM EGTA, 0.15 M NaCl, 5 μg/ml aprotinin, 5 μg/ml leupeptin, 0.5 mM PMSF, 2 mM sodium orthovanadate and 1% SDS. The lysed solution was used for identifying mitochondrial Cyt *c* by immunoblotting. The supernatants were centrifuged at 100,000*g* for 15 min at 4°C, and the obtained supernatants were used for identification of cytosolic cytochrome *c* by immunoblotting.

Analysis of ROS production

The endogenous ROS level was detected by flow cytometry using DCHF-DA.[23] DCHF-DA is a stable fluorescent ROS-sensitive compound, which readily diffuses into cells. DCHF-DA is hydrolyzed by esterase to form DCHF within cells, which is oxidized by hydrogen peroxide or low-molecular-weight peroxides to produce the fluorescent compound 2′,7′-dichlorofluorescein (DCF). In the present study, COLO205 cells were treated with GOS (5 μM) for 1 hr, followed by staining with DCHF-DA (100 μM) for an additional 30 min. Green fluorescence in cells under different treatments was analyzed by flow cytometry analysis.

Analysis of respective caspases activity

Ac-DEVD-pNA for caspase 3, Ac-YVAD-pNA for caspase 1, Ac-VEID-pNA for caspase 6, Ac-IETD-pNA for caspase 8 and Ac-LEHD-pNA for caspase 9 were used as colorimetric substrates for the indicated caspases. Briefly, cells under different treatments were collected and suspended in lysis buffer (50 mM Tris-HCl (pH 7.4), 1 mM EDTA and 10 mM ethyleneglycoltetraacetic acid) for protein extraction. Cell lysates (50 μg) were incubated with 100 μM of the indicated colorimetric substrates at 37°C for 1 hr, and the activity of each caspase was detected by measuring the release of pNA colorimetric materials at a wavelength of 405 nm.

Ethidium bromide treatment of COLO205 cells

Mitochondria were impaired in COLO205 (EtBr-205) cells by culturing cells in routine growth medium supplemented with a dose of EtBr (50 ng/ml) with pyruvate (1 mM) and uridine (50 pg/ml) for 4 weeks.[24,25] Cells were assayed for NADH-ferricyanide reductase activity and cyanide-sensitive oxygen uptake to confirm the loss of mitochondrial function.

Measurement of the mitochondrial membrane potential

COLO205 cells under different treatments were incubated with 40 nM DiOC6(3) for 15 min at 37°C, followed by washing with

ice-cold PBS, after which the cell pellets were collected. Pellets were suspended in 500 μl of PBS, and the fluorescent intensities of cells were analyzed by flow cytometry (FACScan, Becton Dickinson, San Jose, CA), at respective wavelengths for excitation and emission of 484 and 500 nm.

In vivo *antitumor effect of gossypol*

Male BALB/c-nu mice were purchased from the National Laboratory Animal Center of Taiwan. The mice were maintained under Specific Pathogen-Free (SPF) conditions, and supplied with sterilized food and water. The COLO205 cells (5×10^6/0.2 ml) were subcutaneously injected into the flanks of BALB/c-nu mice (4–6 weeks old, 16–20 g in body weight). Once the tumor had reached a volume of 200 mm^3, the mice were randomly divided randomly into five groups, with twelve mice in each group. GOS and GAA stock solutions were prepared at the dose of 100 mg/ml in 20% DMSO, and diluted to the injection doses (5 and 10 mg/kg) by adding PBS. Mice were injected intra-peritoneally (i.p.) with GOS and GAA once a day in 14 consecutive days. At the end of the experiment, the tumors were excised and weighed.

Flow cytometry analysis

COLO205 cells under different treatments were trypsinized, washed with ice-cold PBS, and then fixed in 70% ethanol at –20°C for 1 hr. After fixation, cells were washed twice, followed by incubation in 0.5 ml of 0.5% Triton X-100/PBS containing RNase A (1 mg/ml) at 37°C for 30 min. Cells were stained with 0.5 ml of 50 mg/ml propidium iodide for 10 min, and the DNA content of cells was quantified by FACScan flow cytometry (Becton Dickenson).

Plasmid digestion assay

pBR322 plasmid DNA was used to examine the ROS-producing and scavenging activities of GOS. To analyze the ROS-producing activity of GOS, pBR322 plasmid DNA (0.25 μg) was incubated with different concentrations (25–200 μM) of GOS for 30 min. When detecting the ROS-scavenging activity of GOS and GAA, pBR322 plasmid DNA (0.25 μg) was incubated with different concentrations (25–200 μM) of GOS or GAA in the presence of ROS-producing components (H_2O_2 plus Fe^{+2}) for 30 min. At the end of both reactions, samples were incubated with 5× tracking dye (40 mM EDTA, 0.05% bromophenol blue and 50 % glycerol) to stop the reaction, and the conformation of pBR322 plasmid DNA was analyzed by agarose electrophoresis via EtBr staining, and visualized under UV transilluminator.[17]

Statistical analysis

Values are expressed as the mean ± S.E. A significant difference from the respective controls for each experimental test condition was assayed using Student's *t*-test for each paired experiment. A p-value of < 0.01 or < 0.05 was regarded as indicating a significant difference.

Results

GOS effectively reduces the viability of colorectal carcinoma cells via induction of apoptosis

The chemical structure of GOS has been shown in the upper panel of Figure 1*a*. Thirteen carcinoma cell lines, including HT29, COLO205, COLO320HSR, COLO320DM, HL-60, Jurkat, RAW 264.7, J774A.1, NIH3T3, A431, HaCaT, Glioma C6 and MCF-7, were used to examine the cytotoxic effect of GOS. Results of the MTT assay showed that GOS exhibited dose-dependent cytotoxicity in all tested cell lines, and the IC_{50} values of GOS in HT29, COLO205, COLO320HSR, COLO320DM, HL-60, Jurkat, RAW264.7, J774A.1, NIH3T3, A431, HaCaT, Glioma C6 and MCF-7 cells were 5.3, 3.2, 7.5, 3.4, 9.6, 9.5, 12.5, >20, 20.5, >20, >20, 7.3 and 9.2 μM (Lower panel; Fig. 1*a*). This indicates that colorectal carcinoma cells COLO205, HT29, COLO320HSR and COLO320DM were more sensitive to GOS treatment than other tested cells. These data suggest that GOS exhibits quite-specific cytotoxic effects in colorectal carcinoma cells. To identify if the GOS-induced reduction in viability of colorectal carcinoma cell occurs via apoptosis, both HT29 and COLO205 cells were treated with GOS (5 μM) for different times, and the integrity of DNA and apoptotic morphology were examined by DNA electrophoresis and microscopic observations, respectively. Results of the microscopic observation showed that GOS (5 μM) induced the occurrence of apoptotic bodies in both COLO205 and HT29 cells (data not shown). Data of the MTT assay showed that GOS time-dependently reduced the viability of COLO205 and HT29 cells (Fig. 1*b*). Results of DNA electrophoresis showed that GOS stimulated DNA fragmentation in a dose-dependent manner (Fig. 1*c*), and GOS at a dose of 5 μM time-dependently induced DNA fragmentations in both cells (Fig. 1*d*). GOS showed no effect on the integrity of DNA in either NIH3T3 or HaCaT cells (Fig. 1*e*). These results support GOS reducing the viability of colorectal carcinoma cells via apoptosis induction.

Activation of caspase 3, 6, 8 and 9 enzymes is involved in GOS-induced apoptosis in human colorectal carcinoma cells

It is important to investigate if activation of caspases is essential for GOS-induced apoptosis. Several specific peptidyl substrates for the indicated caspases including caspase 1 substrate Ac-YVAD-pNA, caspase 3 substrate Ac-DEVD-pNA, caspase 6 substrate Ac-VEID-pNA, caspase 8 substrate Ac-IETD-pNA and caspase 9 substrate Ac-LEHD-pNA were used in the study. Results of Figures 2*a* and 2*b* show that the enzyme activities of caspase 3, 6, 8 and 9, but not caspase 1, were increased in a time-dependent manner in both COLO205 and HT29 cells. COLO205-X was cultured from tumors elicited by a subcutaneous (s.c.) injection of COLO205 cells in nude mice, and our study showed that COLO205-X cells possess more-effective migration ability and higher MMP-2 production than those in COLO205 cells.[26] GOS treatment significantly decreased the viability of COLO205-X cells in accordance with the induction of DNA fragmentation, and the IC_{50} value was <10 μM (data not shown). Time-dependent increases in the enzyme activities of the respective caspase 3, 6, 8 and 9 were also identified in GOS-treated COLO205-X cells (Fig. 2*c*). To identify if the activation of caspase 3, 6, 8 and 9 enzyme is essential for GOS-induced apoptosis, the specific peptidyl inhibitors of the indicated caspases were applied in the present study. The addition of Z-VAD-FMK (a broad caspases' inhibitor), Ac-DEVD-FMK (an inhibitor of caspase 3-like protease), and Ac-VEID-FMK (an inhibitor of caspase 6-like protease) fully prevented COLO205 and HT29 cells from GOS-induced DNA fragmentation and cytotoxicity in COLO205 cells according to DNA electrophoresis and the MTT assay, respectively (Figs. 2*d* and 2*e*). However, both Ac-IETD-FMK (an inhibitor of caspase 8-like protease) and Ac-LEHD-FMK (an inhibitor of caspase 9-like protease) respectively attenuated but did not fully block GOS-induced DNA ladder formation and cytotoxicity in COLO205 cells. A complete prevention of GOS-induced DNA ladder formation and cytotoxicity was observed in Ac-IETD-FMK plus Ac-LEHD-FMK-treated COLO205 cells (Figs. 2*d* and 2*e*). These data suggested that GOS-induced apoptosis occurs through activation of caspase 3, 6, 8 and 9 in colorectal carcinoma cells.

Involvement of ROS production upstream of caspase activation in GOS-treated colorectal carcinoma cells

In vitro plasmid digestion provides an effective method to analyze the prooxidant and antioxidant effect of chemicals. In the presence of ROS production, plasmid DNA is damaged and conversion of the plasmid conformation from a supercoiled form (SC) to an open circle (OC) occurs. To analyze if GOS possesses the ability to scavenge ROS production, supercoiled pBR322 plasmid DNA was incubated with H_2O_2 and Fe^{+2} (H_2O_2/Fe^{+2}) with or without different doses (25, 50, 100 and 200 μM) of GOS or GAA for 30 min, and the conformation of the plasmid DNA was ana-

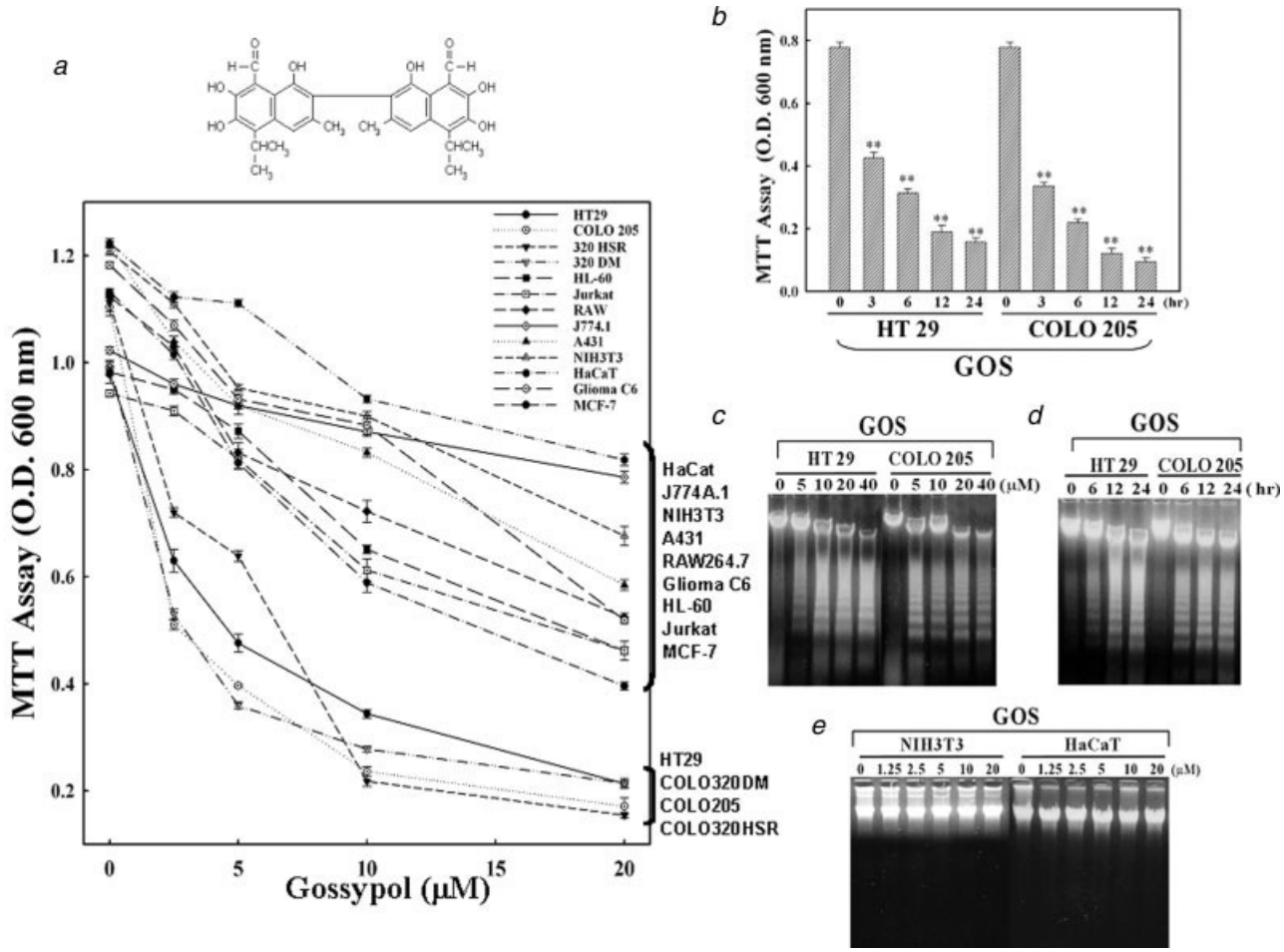

FIGURE 1 – GOS effectively reduced the viability of colorectal carcinoma cells via apoptosis induction. (*a*) The chemical structure of GOS has been shown in the upper panel. The cytotoxic effects of GOS on different carcinoma cells were detected by the MTT assay. Each cell line (1×10^6 cells/well) was plated into 24-well plates for 24 hr and then treated with different concentrations of GOS (2.5, 5, 10 and 20 μM) for a further 24 hr. MTT was added into the medium at the end of incubation for a further 4 hr. The viability of cells was detected by the MTT assay through measuring the absorbance at a wavelength of 600 nm. Each value is presented as the mean ± S.E. of three independent experiments. (*b*) GOS time-dependently reduced the viability of COLO205 and HT29 cells according to the MTT assay. HT29 and COLO205 cells were plated into 24-well plates for 24 hr and then treated with GOS (5 μM) for different times. MTT was added at the end of the indicated times and incubated for a further 4 hr. Each value is presented as the mean ± S.E. of three independent experiments. $^{**}p < 0.01$ significantly different from the control group as analyzed by Student's *t*-test. (*c*) GOS dose-dependently induced DNA ladder formation in HT29 and COLO205 cells. HT29 and COLO205 cells were treated with different concentrations (0, 5, 10, 20 and 40 μM) of GOS for 24 hr and the integrity of DNA was analyzed by agarose electrophoresis through staining with EtBr. (*d*) GOS time-dependently induced DNA ladders in HT29 and COLO205 cells. Both cell lines were treated with GOS (5 μM) for different times (0, 6, 12 and 24 hr), and the integrity of DNA under different treatments was analyzed as described in (*c*). (*e*) No significant DNA ladder was observed in GOS-treated NIH3T3 or HaCaT cells. NIH3T3 and HaCaT cells were treated with different concentrations (0, 1.25, 2.5, 5, 10 and 20 μM) of GOS for 24 hr, and the integrity of DNA was analyzed as described in (*c*).

lyzed by agarose electrophoresis. In the control group, the conformation of pBR322 plasmid is kept in SC form (C). As illustrated in Figure 3*a*, H_2O_2/Fe^{+2} addition induced the conversion of plasmid from SC to OC (+), and neither GOS nor GAA, at the doses form 25 to 200 μM, exhibited a preventive effect against the H_2O_2/Fe^{+2}-induced SC-to-OC conformational changes. Interestingly, GOS and GAA alone dose-dependently induced the conversion of plasmid DNA from SC to OC conformation (Fig. 3*b*). This suggests that GOS exhibits ROS-producing activity *in vitro*. Furthermore, application of antioxidants including NAC, CAT, TEM and MEL significantly reduced the cytotoxicity induced by GOS according to the MTT assay (Fig. 3*c*). Attenuation of GOS-induced DNA ladders was also identified in NAC-, CAT-, TEM- and MEL-treated COLO205 cells (Fig. 3*d*). We further examined if GOS induces ROS production in COLO205 cells by the DCHF-DA assay. Data from the DCHF-DA assay showed that an increase in the intracellular peroxide level was detected in GOS-treated COLO205 cells, and the addition of NAC, CAT, or TEM significantly suppressed the peroxide level induced by GOS (Fig. 3*e*). The protein expression of caspases, PARP and Bcl-2 family proteins in GOS-treated COLO205 cells with or without NAC and TEM treatment was analyzed by Western blotting using specific antibodies in the present study. As illustrated in Figure 3*f*, GOS-induced increases in cleaved PARP and caspase 3 protein, and decreases in pro-caspase 3, 6, 8 and 9 protein expressions in COLO205 cells, and these were blocked by the addition of NAC and TEM. As with Western blotting, a decrease in the Bcl-$_{xL}$ protein and an increase in phosphorylated Bad protein were detected in GOS-treated COLO205 cells, and both events were prevented by the addition of NAC and TEM (Fig. 3*f*). Allopurinol (ALL; a xanthine oxidase inhibitor), PDTC, and DPI (an NADPH oxidase inhibitor) produced no inhibitory effects on GOS-induced apoptotic events or ROS production in GOS-treated COLO205 cells. The protein expression of pro-apoptotic Bax, and antiapoptotic Bag (Bcl-2-associated antideath gene) was not affected by GOS treatment in COLO205 cells. These data supported ROS pro-

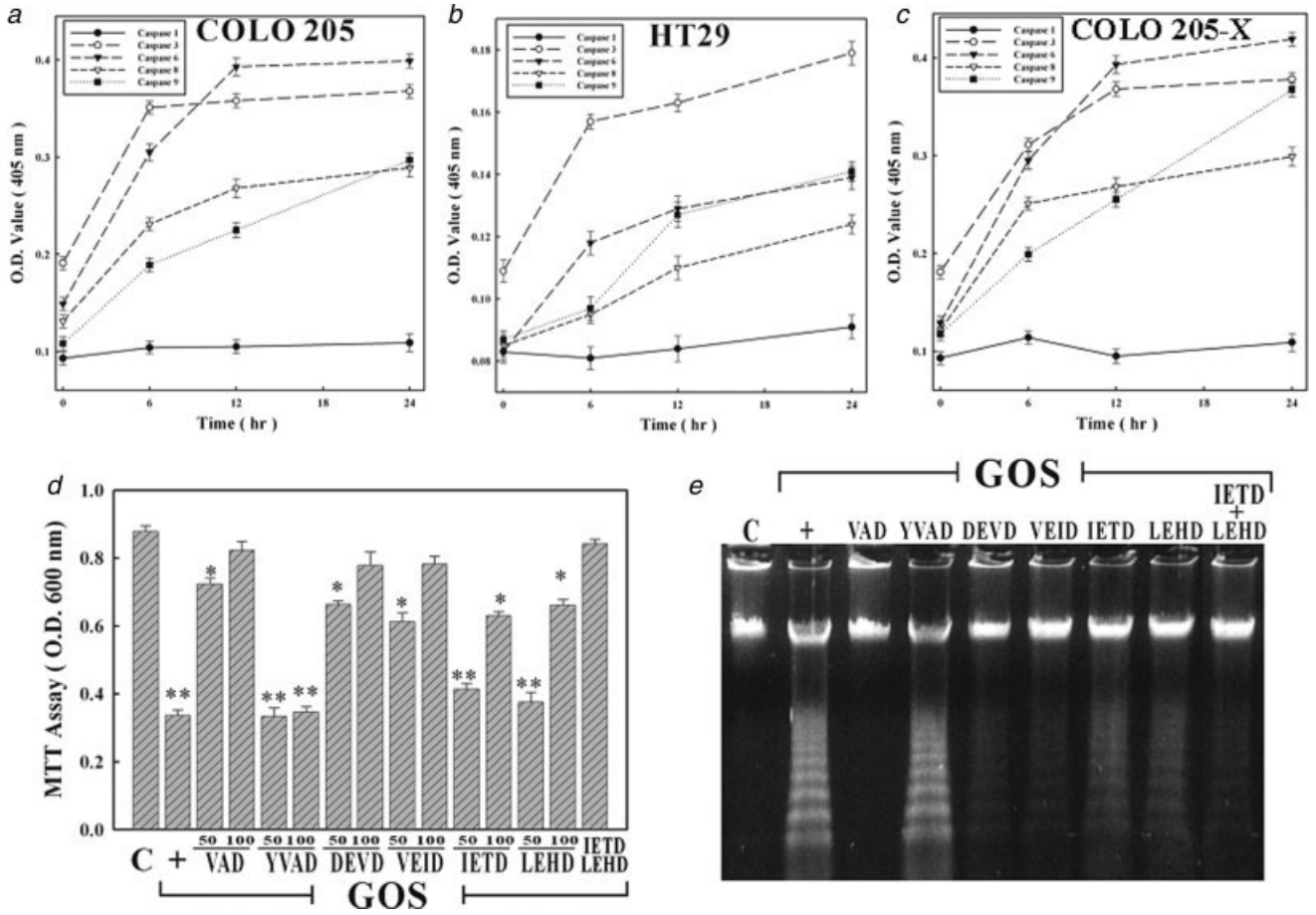

FIGURE 2 – Activation of caspases is involved in GOS-induced apoptosis in human colorectal carcinoma cells. (*a*) Induction of the enzyme activities of caspase 3, 6, 8 and 9 but not caspase 1 enzyme activity in GOS-treated COLO205 cells. Cells were treated with GOS (5 μM) for different time points, and the indicated enzyme activities of caspase 1, 3, 6, 8 and 9 were detected using specific colorimetric substrates as described in the section of "Materials and Methods." Each value is presented as the mean ± SE of three independent experiments. (*b*) As described in (*a*), the indicated caspase activity induced by GOS in HT29 cells was analyzed. (*c*) As described in (*a*), the indicated caspase activity in GOS-treated COLO205-X cells was analyzed. (*d*) Differential protective effects of inhibitors of indicated caspases on GOS-induced apoptosis. COLO205 cells were treated with 50 or 100 μM of Ac-YVAD-FMK, Ac-DEVD-FMK, Ac-VEID-FMK, Ac-IETD-FMK, Ac-LEHD-FMK, or Z-VAD-FMK for 3 hr followed by GOS (5 μM) for a further 24 hr. The viability of cells under different treatments was examined by the MTT assay. $*p < 0.05$, $**p < 0.01$ significantly different from the control group as analyzed by Student's *t*-test. (*e*) As described in (*d*), COLO205 cells were treated with 100 μM of Ac-YVAD-FMK, Ac-DEVD-FMK, Ac-VEID-FMK, Ac-IETD-FMK, Ac-LEHD-FMK, or Ac-VAD-FMK for 3 hr followed by GOS (5 μM) for a further 24 hr. The DNA fragmentation analysis was performed by 1.8% agarose electrophoresis.

duction participating in GOS-induced apoptosis and being located upstream of caspase activation in colorectal carcinoma cells.

Mitochondria are targets for GOS-induced apoptosis in colorectal carcinoma cells

We further examined the effect of GOS on the mitochondrial function of colorectal carcinoma cells. As both AIF and Cyt c are mitochondrial proteins, we investigated if GOS treatment induces the translocation of AIF and Cyt c from mitochondria to the cytoplasm. As illustrated in Figure 4*a*, a time-dependent release of AIF and Cyt c proteins from mitochondria to the cytosol was identified in GOS-treated COLO205 cells by Western blotting (Fig. 4*a*). Translocation of the AIF and Cyt c protein from mitochondria to the cytosol was inhibited by the addition of antioxidants, NAC and TEM (Fig. 4*b*). In addition, the mitochondrial membrane potential was detected by flow cytometry using $DiOC_6(3)$ as a fluorescent dye. The mitochondrial membrane potential in normal cells is located between 20 and 200 DiOC6 fluorescent units (X-axis), therefore the cells located below 20 DiOC6 fluorescent units (M1) are described as the cells with losses of mitochondrial membrane potential. Data of Figure 4*c* show that a decrease in the mitochondrial membrane potential was detected in GOS-treated COLO205 cells, which was blocked by the addition of the antioxidants, NAC, TEM and CAT. These data suggest that GOS-induced apoptosis is mediated by reducing the mitochondrial membrane potential through stimulating ROS production. As described in the section of Materials and Methods, a low dose of EtBr treatment for a long time results in mitochondrial dysfunction by impairing mitochondrial DNA (mtDNA). Therefore, COLO205 cells without mitochondria (EtBr-COLO205) were established in the present study via low-dose of EtBr (50 ng/ml) treatment for 4 weeks, and the apoptotic effect of GOS in parental COLO205 and EtBr-205 cells were examined in the present study. Results of the MTT assay showed that GOS was less effective in EtBr-COLO205 cells than in parental COLO205 cells, and the IC_{50} values of GOS in COLO205 and EtBr-COLO205 cells were 0.98 and 8.14 μM, respectively (Fig. 4*d*). In the same part of the experiments, data from the DNA fragmentation assay showed that GOS-induced DNA ladders were detected in COLO205 cells but not observed in EtBr-205 cells (Fig. 4*f*). Results for DCHF-DA showed that an increase in the intracellular peroxide level was detected in GOS-treated COLO205 cells, but not in EtBr-205 cells (Fig. 4*e*). Association of Fas and Fas ligand (Fas L) are thought to induce apopto-

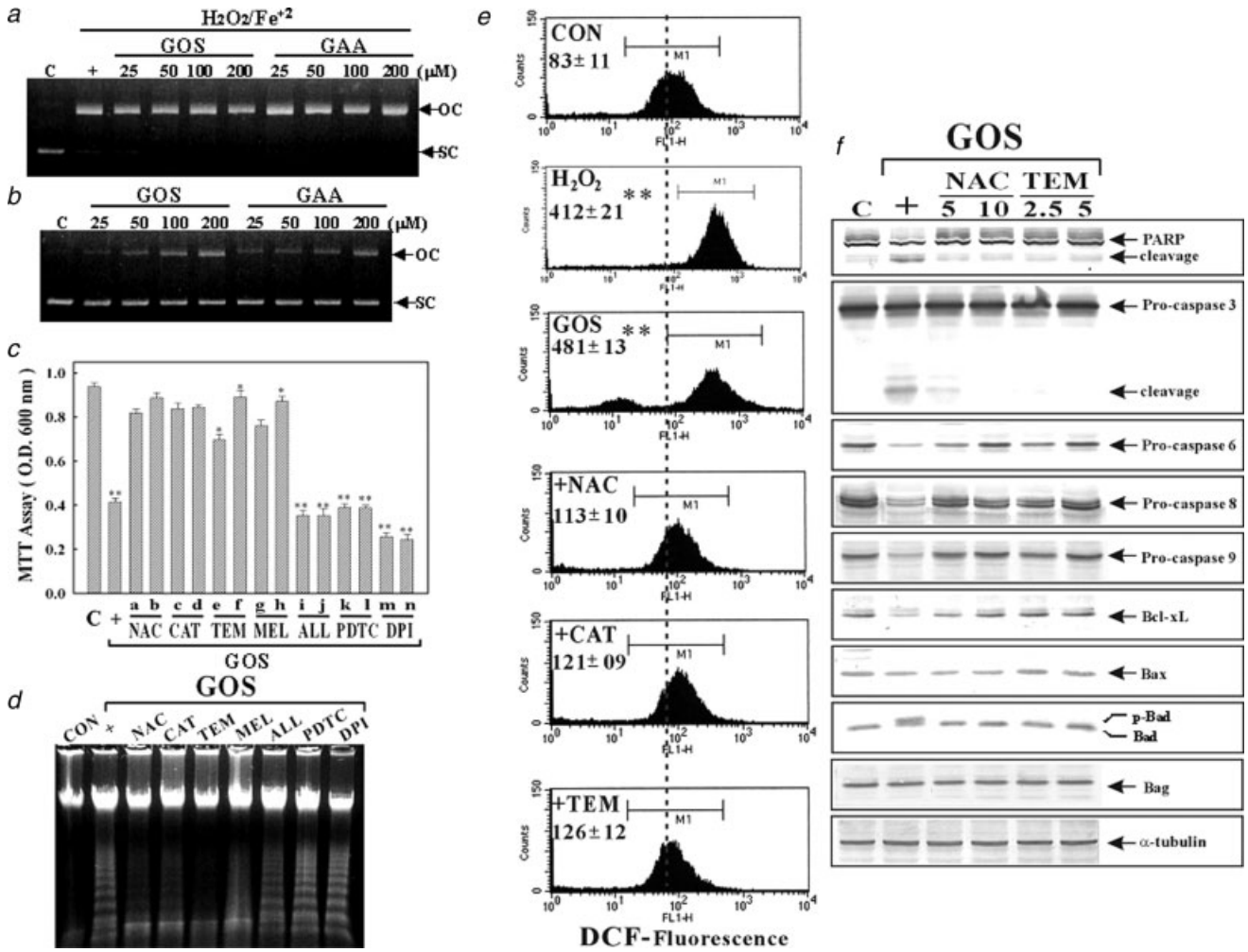

FIGURE 3 – GOS stimulation of ROS production in COLO205 cells. (*a*) GOS did not reduce the H_2O_2/Fe^{+2}-induced ROS production by the *in vitro* plasmid digestion assay. As described in the section of "Materials and Methods," pBR322 plasmid was treated with indicated doses (25, 50, 100 and 200 μM) of GOS or GAA in the presence of H_2O_2/Fe^{+2} for 30 min, and the conformation of the pBR322 plasmid DNA was analyzed by agarose electrophoresis. SC, super-coiled form; OC, open circle form; +, H_2O_2/Fe^{+2}-treatment alone. (*b*) GOS and GAA alone induced the conversion of plasmid DNA from the SC to the OC form. As described in (*a*), pBR322 plasmid DNA was incubated with the indicated doses (25, 50, 100 and 200 μM) of GOS or GAA without H_2O_2/Fe^{+2} for 30 min, and the conformational change of the pBR322 plasmid DNA was analyzed. (*c*) NAC, CAT, TEM and MEL, but not ALL, PDTC, or DPI, inhibited GOS-induced cytotoxic effects in COLO205 cells. Cells were treated with different doses of NAC (a: 5 mM; b: 10 mM), CAT (c: 200 U/ml; d: 400 U/ml), TEM (e: 2.5 μM; f: 5 μM), MEL (g: 50 μM; h: 100 μM), ALL (i: 50 μM; j: 100 μM), PDTC (k: 20 μM; l: 40 μM) or DPI (m: 2.5 μM; n: 5 μM) for 1 hr followed by GOS (5 μM) treatment for a further 24 hr, and the viability of cells was analyzed by the MTT assay. Each value is presented as the mean ± S.E. of three independent experiments. $*p < 0.05$ and $**p < 0.01$ significantly different from the control as analyzed by Student's *t*-test. (*d*) NAC, CAT, TEM and MEL addition attenuated GOS-induced DNA ladder formation in COLO205 cells. As described in (*c*), COLO205 cells were treated with NAC (10 mM), CAT (400 U/ml), TEM (5 μM), MEL (100 μM), ALL (100 μM), PDTC (40 μM) or DPI (5 μM) for 1 hr followed by GOS (5 μM) treatment for further 24 hr, and the integrity of DNA was analyzed by agarose electrophoresis as described in the section of "Material and Methods." (*e*) An increase in the intracellular peroxide level was observed in GOS-treated COLO205 cells. Cells were treated with GOS (5 μM) for 1 hr in the presence or absence of a prior 1-hr incubation with NAC (10 mM), CAT (400 U/ml) and TEM (5 μM). DCHF-DA was added into each sample for 30 min, and the DCF fluorescence intensity in cells was detected by flow cytometry analysis. Each value is presented as the mean ± S.E. of three independent experiments. $**p < 0.01$ significantly different from the control as analyzed by Student's *t*-test. (*e*) Alternative expression of caspases and Bcl-2 family protein in GOS-treated COLO205 cells. Cells were treated with different concentrations of NAC (5 and 10 mM) or TEM (2.5 and 5 μM) for 1 hr followed by GOS (5 μM) treatment for a further 24 hr. Expression of pro-caspases, cleavage of PARP and Bcl-2 family proteins such as Bcl-xL, Bax, Bad and Bag were detected by western blotting.

sis through an mitochondria-independent processes. To investigate if EtBr treatment specifically affects mitochondrial function, the DX2 antihuman Fas antibody was used in the present study to mimic the role of Fas L, and Griffith *et al*. have shown that cross-linking with DX2 delivers an apoptotic signal in cells.[27] As illustrated in Figure 4*g*, application of DX2 antihuman Fas antibody induces DNA ladder formation in both COLO205 and EtBr-205 cells (Fig. 4*g*). It indicates that EtBr treatment may not interfere mitochondria-independent apoptotic pathway elicited by Fas activation. These data provide evidences to indicate a mitochondria-dependent apoptosis by GOS in colorectal carcinoma cells.

In vivo *anticolorectal carcinoma effect of GOS in nude mice*

The *in vivo* anticolorectal carcinoma effect of GOS is still undefined. In previous studies, we established an *in vivo* nude mice model to screen for effective anticolorectal carcinoma agents.[23] Nude mice were subcutaneously injected with COLO205 cells

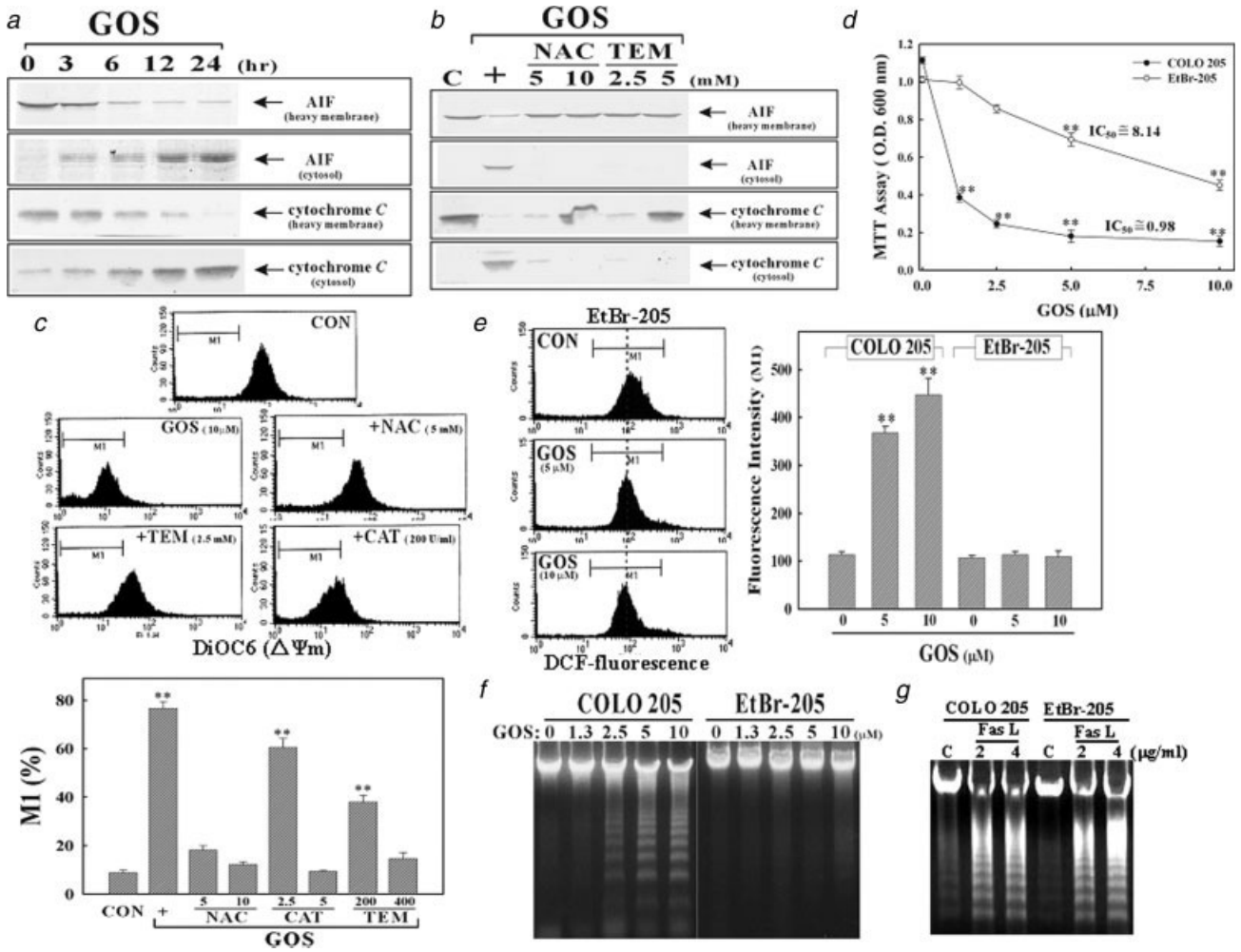

FIGURE 4 – The GOS-induced apoptosis through a mitochondrial pathway. (*a*) GOS time-dependently induced the translocation of the mitochondrial proteins AIF and cytochrome c (Cyt c), to the cytosol. COLO205 cells were treated with GOS (5 μM) for different times (3, 6, 12 and 24 hr), and the cytosolic and heavy membrane fractions were prepared. The expressions of AIF and Cyt c protein in both fractions were detected by Western Blotting. (*b*) NAC and TEM inhibited the GOS-induced AIF and Cyt c protein translocation in COLO205 cells. Cells were treated with different concentrations of NAC (5 and 10 mM) or TEM (2.5 and 5 μM) for 1 hr followed by GOS (5 μM) treatment for a further 24 hr. The release of AIF and Cyt c protein from mitochondria to the cytosol was analyzed by Western blotting. (*c*) NAC, CAT and TEM significantly reduced the loss of the mitochondrial membrane potential (MMP, $\Delta\Psi_m$) induced by GOS. COLO205 cells were treated with NAC, CAT, or TEM for 1 hr followed by GOS (5 μM) treatment for a further 12 hr. At the end of treatment, $DiOC_6(3)$ was added to the culture medium for a further 30 min. The fluorescence intensity of $DiOC_6(3)$ in cells was analyzed by flow cytometry. (Upper panel) A representative of data of the flow cytometric analysis; (Lower panel) Quantification of M1 values from three-independent experiments was performed, and results are expressed as the mean ± S.E. $^{**}p < 0.01$ significantly different from the control as analyzed by Student's *t*-test. (*d*) EtBr-treated COLO205 cells (EtBr-205; mitochondria-depleted, p^0 cells) possessed resistance to GOS-induced cytotoxicity, compared with parental COLO205 cells. EtBr-205 and parental COLO205 cells were treated with different doses of GOS (1.25, 2.5, 5 and 10 μM) for 24 hr, and the viability of cells was measured by the MTT assay. $^{**}p < 0.01$ significantly different from the control as analyzed by Student's *t*-test. (*e*) GOS did not induce ROS production in EtBr-205 cells according to the DCHF-DA assay. Both parental COLO205 and EtBr-205 cells were incubated with different doses (5 and 10 μM) of GOS for 1 hr, followed by DCHF-DA addition for 30 min. The DCF fluorescence intensity in cells was detected by flow cytometry analysis. (Left panel) A representative of data of the flow cytometric analysis; (Right panel) Values of M1 derived from three-independent experiments were analyzed, and results are presented as the mean ± S.E. $^{**}p < 0.01$ significantly different from the control as analyzed by Student's *t*-test. (*f*) GOS (5 μM) did not induce DNA ladders in ErBr-205 cells. Both parental COLO205 and EtBr-205 cells were incubated with different doses (1.3, 2.5, 5 and 10 μM) for 24 hr, and the integrity of DNA was analyzed. (*g*) The addition of DX2 antihuman Fas antibody induced DNA ladder formation in both COLO205 and EtBr-205 cells. Both cells were treated with DX2 antihuman Fas antibody (2 and 4 μg/ml) for 24 hr, and the integrity of DNA was analyzed.

followed by an i.p. injection of GOS or GAA (5 or 10 mg/kg) when the tumor volume had reached 200 mm^3. Results in Figure 5*a* showed that GAA possessed significant apoptosis-inducing activity in both COLO205 and HT29 cells, and DNA ladders induced by GAA were detected in time- and dose-dependent manners in both cells. The respective IC_{50} values of GAA in COLO205 cells and HT29 cells were 3.4 and 5.1 μM, respectively. Results of the *in vivo* study showed that both GOS and GAA significantly reduced tumor growth in nude mice elicited by an s.c. injection of COLO205 cells, compared with the vehicle-treated groups. GAA, at a dose of 5 mg/kg, showed more-significant reduction on the growth of tumors than GOS (Figs. 5*b* and 5*c*).

Discussion

Although apoptosis induced by GOS was previously proposed, we provide additional scientific evidence indicating that induction

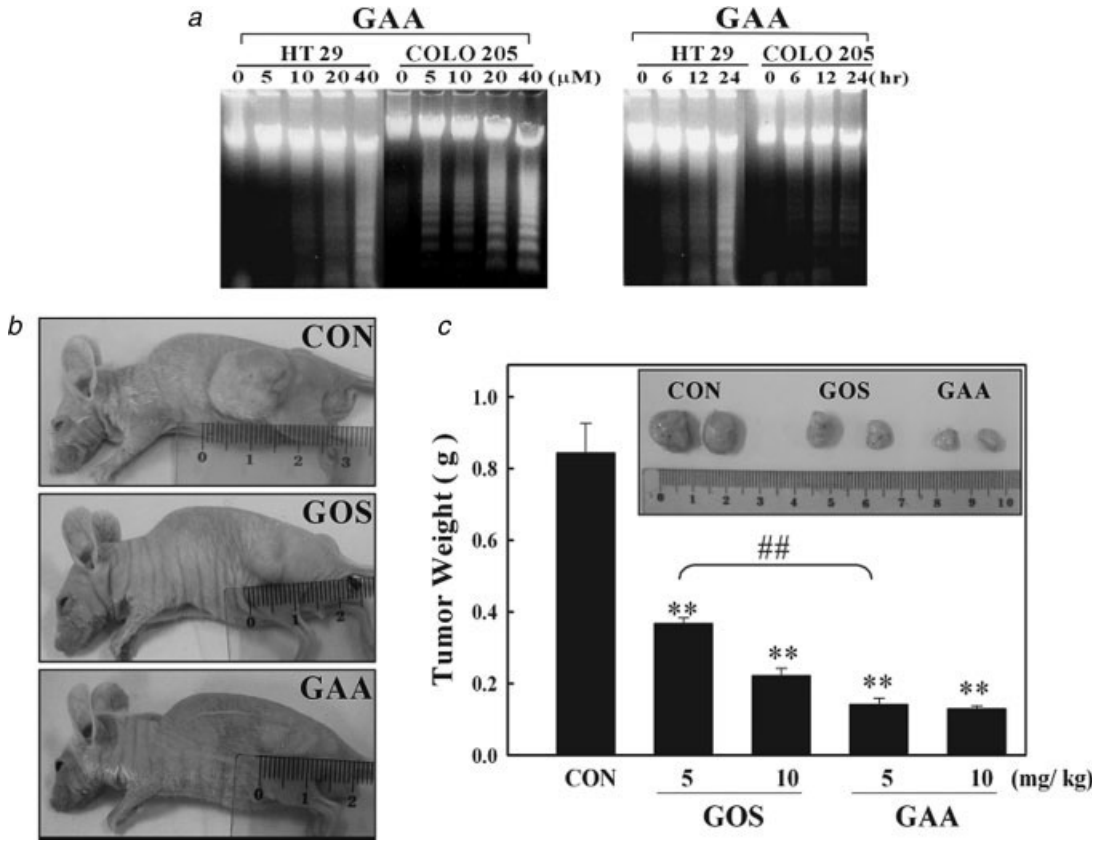

FIGURE 5 – GOS and GAA suppression of tumor growth in nude mice elicited by a subcutaneous injection of COLO205 cells. (*a*) (Left panel) GAA dose-dependently induced DNA ladders in HT29 and COLO205 cells. Both cell lines were treated with different concentrations (5, 10, 20 and 40 μM) of GAA for 24 hr and the integrity of DNA was analyzed. (Right panel) GAA time-dependently induced DNA ladders in HT29 and COLO205 cells. Both cell lines were treated with GAA (5 μM) for different times (0, 6, 12 and 24 hr), and the integrity of DNA in both cell lines was analyzed. (*b*) GOS and GAA reduced tumor growth *in vivo*. The protocol of *in vivo* study has been described in the section of Materials and Methods. GOS and GAA (5 and 10 mg/kg) were intraperitoneally injected once a day for 14 consecutive days. Representatives of nude mice derived from the vehicle (CON), GOS- (10 mg/ml) and GAA- (10 mg/kg)-treated groups are shown. At the end of the experiment, tumors were excised from the nude mice under different treatments, and representatives of isolated tumors from the control-, GOS-, and GAA-treated groups are shown (Upper panel). (Lower panel) The mean value of tumor weight in each group was measured at the end of the experiment, and results are expressed as the means ± S.E. $^{**}p < 0.01$ indicates significant differences from the control group; $\#\#p < 0.01$ indicates significant differences between indicated groups, as analyzed by Student's *t*-test.

of ROS production is an important event in GOS-induced apoptosis and that it is located upstream of mitochondrial dysfunction and caspase activation. This suggests that the antitumor effect of GOS is mediated by the induction of apoptosis via an ROS-dependent mitochondrial pathway in colorectal carcinoma cells.

GOS has been shown to reduce the viability of different tumor cells including leukemia, fibrosarcoma, breast cancer, colon carcinoma, cervical cancer, glioma and melanoma.[28–30] Mego indicated that GOS was a potential telomerase inhibitor, and posited that the use of GOS with other anticancer chemotherapeutics could lead to an effective therapy for human tumors.[31] Ligueros *et al*. suggested that modulation of cell cycle progression was involved in GOS-induced growth inhibition.[32] In prostate cancers, GOS inhibited the growth of prostate cancer cells by arresting cells in the G0/G1 phase.[33] However, a low response of GOS against malignant glioma[34] and a negligible antitumor effect against refractory metastatic breast cancer were reported.[35] Data of the present study show that colorectal carcinoma cells expressed higher sensitivity to GOS treatment than others including HL-60, Jurkat, RAW264.7, J774A.1, NIH3T3, A431, HaCaT, Glioma C6 and MCF-7 cells. COLO205 and HT29 cells respectively belong to poorly and modest/well differentiated colorectal carcinoma cells with different p53 status. The p53 in HT29 cells has been shown to be a mutated protein with a mutation at codon 273,[36] and that in COLO205 is proposed to be functional without mutation.[37] Van Poznak *et al*. proposed that GOS-induced apoptosis was not associated with the regulation of p53,[35] and Zhang *et al*. indicated that no change in p53 protein was observed in GOS-treated HT29 cells.[5] Data of the present study also found that GOS induced apoptosis in both HT29 and COLO205 cells. It is possible that GOS-induced apoptosis was not affected by intracellular p53 status. In addition to p53, Bcl-2 family proteins have been reported to be associated with the mitochondrial membrane potential and caspases activation during apoptosis. The results of the present study indicate that GOS treatment can down-regulate Bcl-$_{xL}$ protein, and up-regulate phospho-Bad protein expression in COLO205 cells. These results are consistent with previous observations in which a decrease in Bcl-$_{xL}$ and an increase in phospho-Bad protein have been shown in GOS-treated HT29 cells.[5]

Mitochondria are involved in the apoptosis signal transduction pathway. Release of Cyt c and AIF from mitochondria to the cytosol, followed by induction of caspase 9-dependent activation of caspase 3, has been identified in the process of mitochondria-dependent apoptosis. Bcl-2 family proteins have been shown to be involved in modulation of mitochondrial membrane potentials (MMPs), and loss of MMPs via decreasing antiapoptotic Bcl-2 family proteins such as Bcl-$_{XL}$ with or without increasing pro-apoptotic Bcl-2 family proteins Bax and Bad has been identified

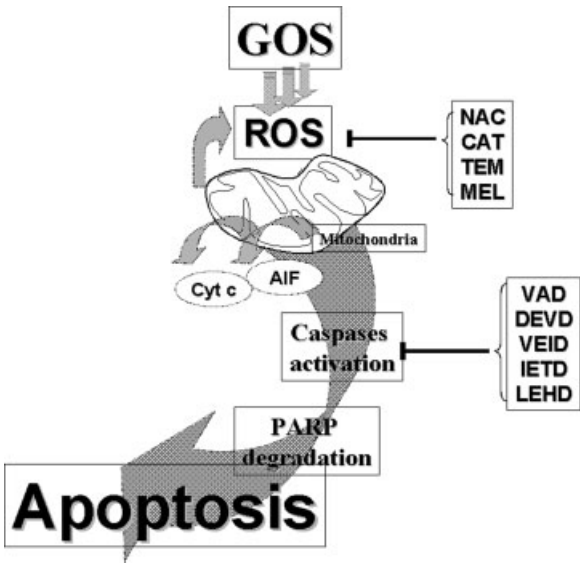

FIGURE 6 – Tentative anticolorectal carcinoma mechanism induced by GOS was proposed in the present study. ROS, reactive oxygen species; GOS, gossypol; NAC, *N*-acetyl-cysteine; CAT, catalase; DPI, diphenylene iodonium; TEM, tempol; MEL, melatonin; Cyt c, cytochrome c; AIF, apoptosis-inducing factor; PARP, poly (ADP ribose) polymerase.

in mitochondria-dependent apoptosis. Kitada *et al*. suggested that GOS is able to directly bind and antagonize their antiapoptotic effects of Bcl-2 family proteins such as Bcl-$_{xL}$.[38] In the present study, a decrease in Bcl-$_{xL}$ and an increase in phospho-Bad protein expression were detected in GOS-treated cells, and EtBr-treated COLO205 cells expressed resistance to GOS-induced apoptosis through a reduction in ROS production. It was confirmed that both caspase 9 activation and AIF/Cyt c release happened after GOS treatment. These results suggest GOS-induces apoptosis of colorectal carcinoma cells is through the mitochondrial pathway. Another apoptotic pathway characterized by activation of the death receptor (Fas/CD95/APO-1) and caspase 8 has also been examined in the present study. Activation of caspase 8 enzyme activity with a decrease in the pro-caspase 8 protein was detected in GOS-treated colorectal carcinoma cells, and it was prevented by the antioxidants NAC and TEM. Application of Ac-IETD-FMK (an inhibitor of caspase 8) significantly but not fully inhibited GOS-induced cytotoxic effect in COLO205 cells. That is, GOS might bind to some death receptors or induce the expression of death ligand such as Fas ligand, which in turn to activate the death receptor signaling transduction pathway. Furthermore, a complete protection of COLO205 cells from GOS-induced apoptosis was observed in the condition with Ac-IETD-FMK plus Ac-LEHD-FMK (an inhibitor of caspase 9-like protease) treatment. This suggests that at least two apoptotic pathways including mitochondral-dependent and death receptors-dependent pathways are involved in GOS-induced apoptosis.

ROS act as secondary messengers in apoptosis induced by anticancer and chemopreventive agents. ROS generation can cause the loss of MMP, and induce apoptosis by releasing pro-apoptotic proteins such as AIF and Cyt c from mitochondria to the cytosol. Hou *et al*. indicated that GOS-induced apoptosis in human promyelocytic leukemia cells occurs through an ROS-independent mitochondrial pathway.[20] In this study, induction of intracellular ROS was detected by DCHF-DA, and chemical antioxidants significantly suppressed GOS-induced apoptosis in accordance with reducing ROS production and preventing the loss of the MMPs. GOS-induced mitochondrial events such as the release of Cyt c and AIF to the cytosol, decreasing Bcl-XL, and increasing phosphor-Bad protein expression were blocked by the antioxidants NAC and TEM. These data suggest that GOS-induced apoptosis occurs through elevation of intracellular ROS production, which is located upstream of mitochondrial dysfunction. Tentative anticolorectal carcinoma mechanism induced by GOS was proposed in the present study (Fig. 6).

Natural GOS is a racemic mixture of two enantiomers, (+)GOS and (−)GOS, and previous studies indicated that (−) GOS is more effective in suppressing cell proliferation and inducing apoptosis than (+) GOS in pancreatic cancer cells.[39] Several GOS metabolites, such as apogossypol hexaacetate, and gossypolone have been identified, and GOS exhibited more-potent antitumor activity than its metabolites.[40–42] GAA, a complex consisting of equimolar quantities of GOS and acetic acid, was used in the study to compare its antitumor effects with those of GOS. Data from the vitro and *in vivo* studies showed that both GOS and GAA are effective in apoptosis induction and tumor growth inhibition in colorectal carcinoma cells. GAA at a dose of 5 mg/kg expressed more potent inhibition on *in vivo* tumor growth than did GOS. The reason why GAA performed a more-effective antitumor effect than GOS *in vivo* is still unclear. Lambert *et al*. have shown that acetylation may increase the *in vitro* biological potency of (−)-epigallocatechin-3-gallate (EGCG), and enhance the bioavailability of EGCG *in vivo*.[43] Haspel *et al*. indicated that serum protein prevented the antiproliferative effect of GOS *in vitro*.[44] It suggests that acetylation and reducing serum binding may be another prospective area in GOS related pre-clinical research.

References

1. Janero DR, Burghardt B. Protection of rat myocardial phospholipid against peroxidative injury through superoxide-(xanthine oxidase)-dependent, iron-promoted Fenton chemistry by the male contraceptive gossypol. Biochem Pharmacol 1988;37:3335–42.
2. Lin TS, Schinazi RF, Zhu J, Birks E, Carbone R, Si Y, Wu K, Huang L, Prusoff WH. Anti-HIV-1 activity and cellular pharmacology of various analogs of gossypol. Biochem Pharmacol 1993;46:251–5.
3. Bauer JA, Trask DK, Kumar B, Los G, Castro J, Lee JS, Chen J, Wang S, Bradford CR, Carey TE. Reversal of cisplatin resistance with a BH3 mimetic, (−)-gossypol, in head and neck cancer cells: role of wild-type p53 and Bcl-xL. Mol Cancer Ther 2005;4:1096–104.
4. Conners R, Schambach F, Read J, Cameron A, Sessions RB, Vivas L, Easton A, Croft SL, Brady RL. Mapping the binding site for gossypol-like inhibitors of Plasmodium falciparum lactate dehydrogenase. Mol Biochem Parasit 2005;142:137–48.
5. Zhang M, Liu H, Guo R, Ling Y, Wu X, Li B, Roller PP, Wang S, Yang D. Molecular mechanism of gossypol-induced cell growth inhibition and cell death of HT-29 human colon carcinoma cells. Biochem Pharmacol 2003;66:93–103.
6. Xu L, Yang D, Wang S, Tang W, Liu M, Davis M, Chen J, Rae JM, Lawrence T, Lippman ME. (−)-Gossypol enhances response to radiation therapy and results in tumor regression of human prostate cancer. Mol Cancer Ther 2005;4:197–205.
7. Bushunow P, Reidenberg MM, Wasenko J, Winfield J, Lorenzo B, Lemke S, Himpler B, Corona R, Coyle T. Gossypol treatment of recurrent adult malignant gliomas. J Neuro Oncol 1999;43:79–86.
8. Shelley MD, Hartley L, Fish RG. Groundwater P, Morgan JJ, Mort D, Mason M, Evans A. Stereo-specific cytotoxic effects of gossypol enantiomers and gossypolone in tumour cell lines. Cancer Let 1999;135:171–80.
9. Zhang Y, Kulp SK, Sugimoto Y, Brueggemeier RW, Lin YC. The (−)-enantiomer of gossypol inhibits proliferation of stromal cells derived from human breast adipose tissues by enhancing transforming growth factor beta1 production. Inter J Oncol 1998;13:1291–7.
10. Teng CS, Vilagrasa X. Biphasic c-Myc protein expression during gossypol-induced apoptosis in rat spermatocytes. Contraception 1998;57:117–23.
11. Teng CS. Gossypol-induced apoptotic DNA fragmentation correlates with inhibited protein kinase C activity in spermatocytes. Contraception 1995;52:389–95.
12. Oliver CL, Miranda MB, Shangary S, Land S, Wang S, Johnson DE. (−)-Gossypol acts directly on the mitochondria to overcome Bcl-2-

and Bcl-X(L)-mediated apoptosis resistance. Mol Cancer Ther 2005;4:23–31.
13. Chang JS, Hsu YL, Kuo PL, Chiang LC, Lin CC. Upregulation of Fas/Fas ligand-mediated apoptosis by gossypol in an immortalized human alveolar lung cancer cell line. Clin Exp Pharmacol Physiol 2004;31:716–22.
14. Hu YF, Chang CJ, Brueggemeier RW, Lin YC. Presence of antitumor activities in the milk collected from gossypol-treated dairy cows. Cancer Let 1994;87:17–23.
15. Li Q, Sato EF, Kira Y, Nishikawa M, Utsumi K, Inoue M. A possible cooperation of SOD1 and cytochrome c in mitochondria-dependent apoptosis. Free Rad Biol Med 2006;40:173–81.
16. Ko CH, Shen SC, Chen YC. Hydroxylation at c4′ or c6 is essential for apoptosis-inducing activity of flavanone through activation of the caspase 3 cascade and production of reactive oxygen species. Free Rad Biol Med 2004;36:897–910.
17. Ko CH, Shen SC, Hsu CS, Chen YC. Mitochondrial-dependent, reactive oxygen species-independent apoptosis by myricetin: roles of protein kinase C, cytochrome c, and caspase cascade. Biochem Pharmacol 2005;69:913–27.
18. Lee ER, Kang YJ, Kim JH, Lee HT, Cho SG. Modulation of apoptosis in HaCaT keratinocytes via differential regulation of ERK signaling pathway by flavonoids. J Biol Chem 2005;280:31498–507.
19. Jung EM, Lim JH, Lee TJ, Park JW, Choi KS, Kwon TK. Curcumin sensitizes tumor necrosis factor-related apoptosis-inducing ligand (TRAIL)-induced apoptosis through reactive oxygen species-mediated upregulation of death receptor 5 (DR5). Carcinogenesis 2005;26: 1905–13.
20. Hou DX, Uto T, Tong X, Takeshita T, Tanigawa S, Imamura I, Ose T, Fujii M. Involvement of reactive oxygen species-independent mitochondrial pathway in gossypol-induced apoptosis. Arch Biochem Biophys 2004;428:179–87.
21. Ko CH, Shen S-C, Lin H-Y, Hou WC, Lee WR, Yang LL, Chen Y-C. Flavanones structure related inhibition on TPA-induced tumor promotion through suppression of extracellular signal-regulated protein kinases: involvement of prostaglandin E2 in anti-promotive process. J Cell Physiol 2002;193:93–10.
22. Shen SC, Ko CH, Hsu KC, Chen YC. 3-OH flavone inhibition of epidermal growth factor-induced proliferation through blocking prostaglandin E_2 production. Int J Cancer 2004;108:502–10.
23. Shen SC, Ko CH, Tseng SW, Tsai SH, Chen YC. Structurally related antitumor effects of flavanones *in vitro* and *in vivo*: involvement of caspase 3 activation, p21 gene expression, and reactive oxygen species production. Toxicol Appl Pharmacol 2004;197:84–95.
24. Felty Q, Singh KP, Roy D. Estrogen-induced G1/S transition of G0-arrested estrogen-dependent breast cancer cells is regulated by mitochondrial oxidant signaling. Oncogene 2005;24:4883–93.
25. Delsite R, Kachhap S, Anbazhagan R, Gabrielson E, Singh KK. Mol Cancer1:6.
26. Ko CH, Shen SC, Lee TJF, Chen YC. Myricetin inhibits matrix metalloproteinase 2 protein expression and enzyme activity in colorectal carcinoma cells. Mol Cancer Ther 2005;4:281–290.
27. Griffith TS, Ferguson TA. The role of FasL-induced apoptosis in immune privilege. Immunol Today 1997;18:240–4.
28. Ligueros M, Jeoung D, Tang B, Hochhauser D, Reidenberg MM, Sonenberg M. Gossypol inhibition of mitosis, cyclin D1 and Rb protein in human mammary cancer cells and cyclin-D1 transfected human fibrosarcoma cells. Br J Cancer 1997;76:21–8.
29. Oliver CL, Bauer JA, Wolter KG, Ubell ML, Narayan A, O'Connell KM, Fisher SG, Wang S, Wu X, Ji M, Carey TE, Bradford CR. *In vitro* effects of the BH3 mimetic, (−)-gossypol, on head and neck squamous cell carcinoma cells. Clin Cancer Res 2004;10:7757–63.
30. Shelley MD, Hartley L, Groundwater PW, Fish RG. Structure-activity studies on gossypol in tumor cell lines. Anticancer Drugs 2000;11: 209–16.
31. Mego M. Telomerase inhibitors in anticancer therapy: gossypol as a potential telomerase inhibitor. Bratislavske Lekarske Listy 2002;103: 378–81.
32. Ligueros M, Jeoung D, Tang B, Hochhauser D, Reidenberg MM, Sonenberg M. Gossypol inhibition of mitosis, cyclin D1 and Rb protein in human mammary cancer cells and cyclin-D1 transfected human fibrosarcoma cells. Br J Cancer 1997;76:21–8.
33. Shidaifat F, Canatan H, Kulp SK, Sugimoto Y, Zhang Y, Brueggemeier RW, Somers WJ, Chang WY, Wang HC, Lin YC. Gossypol arrests human benign prostatic hyperplastic cell growth at G0/G1 phase of the cell cycle. Anticancer Res 1997;17:1003–9.
34. Bushunow P, Reidenberg MM, Wasenko J, Winfield J, Lorenzo B, Lemke S, Himpler B, Corona R, Coyle T. Gossypol treatment of recurrent adult malignant gliomas. J Neurooncol 1999;43:79–86.
35. Van Poznak C, Seidman AD, Reidenberg MM, Moasser MM, Sklarin N, Van Zee K, Borgen P, Gollub M, Bacotti D, Yao TJ, Bloch R, Ligueros M, et al. Oral gossypol in the treatment of patients with refractory metastatic breast cancer: a phase I/II clinical trial. Breast Cancer Res Treat 2001;66:239–48.
36. Nagasawa H, Lin CY, Maki CG, Imrich AC, Little JB. Relationship between radiation-induced G1 phase arrest and p53 function in human tumor cells. Cancer Res 1995;55:1842–6.
37. Chen YC, Kuo TC, Lin-Shiau SY, Lin JK. Induction of HSP70 gene expression by modulation of Ca(+2) ion and cellular p53 protein by curcumin in colorectal carcinoma cells. Mol Carcinogen 1996;17: 224–34.
38. Kitada S, Leone M, Sareth S, Zhai D, Reed JC, Pellecchia M. Discovery, characterization, and structure-activity relationships studies of proapoptotic polyphenols targeting B-cell lymphocyte/leukemia-2 proteins. J Med Chem 2003;46:4259–64.
39. Benz CC, Keniry MA, Ford JM, Townsend AJ, Cox FW, Palayoor S, Matlin SA, Hait WN, Cowan KH. Biochemical correlates of the antitumor and antimitochondrial properties of gossypol enantiomers. Mol Pharmacol 1990;37:840–7.
40. Dao VT, Dowd MK, Martin MT, Gaspard C, Mayer M, Michelot RJ. Cytotoxicity of enantiomers of gossypol Schiff's bases and optical stability of gossypolone. Eur J Med Chem 2004;39:619–24.
41. Baumgrass R, Weiwad M, Erdmann F, Liu JO, Wunderlich D, Grabley S, Fischer G. Reversible inhibition of calcineurin by the polyphenolic aldehyde gossypol. J Biol Chem 2001;276:47914–21.
42. Dao VT, Dowd MK, Gaspard C, Martin MT, Hemez J, Laprevote O, Mayer M, Michelot RJ. New thioderivatives of gossypol and gossypolone, as prodrugs of cytotoxic agents. Bioorgan Med Chem 2003;11: 2001–6.
43. Lambert JD, Sang S, Hong J, Kwon SJ, Lee MJ, Ho CT, Yang CS. Peracetylation as a means of enhancing *in vitro* bioactivity and bioavailability of epigallocatechin-3-gallate. Drug Metab Dispos 2006;34: 2111–6.
44. Haspel HC, Ren YF, Watanabe KA, Sonenberg M, Corin RE. Cytocidal effect of gossypol on cultured murine erythroleukemia cells is prevented by serum protein. J Pharmacol Exp Ther 1984;229:218–25.